Journal of Solid State Chemistry 182 (2009) 3105–3112

Contents lists available at ScienceDirect

Journal of Solid State Chemistry

journal homepage: www.elsevier.com/locate/jssc

Interpenetrating metal-organic frameworks formed by self-assembly of tetrahedral and octahedral building blocks

Yong-Ming Lu, Ya-Qian Lan, Yan-Hong Xu, Zhong-Min Su *, Shun-Li Li *, Hong-Ying Zang, Guang-Juan Xu

Institute of Functional Material Chemistry, Key Laboratory of Polyoxometalate Science of Ministry of Education, Faculty of Chemistry, Northeast Normal University, Changchun 130024, China

ARTICLE INFO

Article history:
Received 24 April 2009
Received in revised form
7 August 2009
Accepted 18 August 2009
Available online 22 August 2009

Keywords:
Metal-organic frameworks
Interpenetration
Molecular building blocks
Topology

ABSTRACT

To investigate the relationship between topological types and molecular building blocks (MBBs), we have designed and synthesized a series of three-dimensional (3D) interpenetrating metal-organic frameworks based on different polygons or polyhedra under hydrothermal conditions, namely $[Cd(bpib)_{0.5}(L^1)]$ (**1**), $[Cd(bpib)_{0.5}(L^2)]\cdot H_2O$ (**2**), $[Cd(bpib)_{0.5}(L^3)]$ (**3**) and $[Cd(bib)_{0.5}(L^1)]$ (**4**), where bpib=1,4-bis(2-(pyridin-2-yl)-1*H*-imidazol-1-yl)butane, bib=1,4-bis(1*H*-imidazol-1-yl)butane, H_2L^1=4-(4-carboxybenzyloxy)benzoic acid, H_2L^2=4,4′-(ethane-1,2-diylbis(oxy))dibenzoic acid and H_2L^3=4,4′-(1,4-phenylenebis(methylene))bis(oxy)dibenzoic acid, respectively. Their structures have been determined by single crystal X-ray diffraction analyses and further characterized by elemental analyses, IR spectra, and thermogravimetric (TG) analyses. Compounds **1**–**3** display α-Po topological nets with different degrees of interpenetration based on the similar octahedral $[Cd_2(-COO)_4]$ building blocks. Compound **4** is a six-fold interpenetrating diamondoid net based on tetrahedral MBBs. By careful inspection of these structures, we find that various carboxylic ligands and N-donor ligands with different coordination modes and conformations, and metal centers with different geometries are important for the formation of the different MBBs. It is believed that different topological types lie on different MBBs with various polygons or polyhedra. Such as four- and six-connected topologies are formed by tetrahedral and octahedral building blocks. In addition, with the increase of carboxylic ligands' length, the degrees of interpenetration have been changed in the α-Po topological nets. And the luminescent properties of these compounds have been investigated in detail.

1. Introduction

The rational design and assembly of metal-organic frameworks (MOFs) with well-regulated network structures have received remarkable attention and have developed rapidly for the sake of developing new functional materials with potential applications in recent years [1–6]. The topological analysis of multitudinous networks has become a topical research area, and is not only an important tool for simplifying complicated compounds but also plays an instructive role in the rational design of certain functional materials with desirable properties [7,8]. To date, network topologies in coordination polymers have been discussed in several notable reviews [9–12] following a seminal compilation by Wells decades ago [13,14]. But true crystal engineering of coordination polymers (i.e. prediction of the solid-state structure precisely) still remains a long-term challenge for the crystal engineers. The crystal engineered nets invoke geometric design principles means that a chemically diverse range of molecular building blocks are available for study as exemplified by coordination polymers [15–21]. Zaworotko has used various vertex-linked polygons or polyhedra (VLPP) method to delineate their well-defined MOFs [22,23]. The simplest MOFs consist of unitary nets with one type of node. The majority unitary nets are based on four- and six-connected topologies [24–29], and the common and important topological types are related to the structure of various diamondoid, and α-Po (the primitive cubic=**pcu** with the $(4^{12}\cdot 6^3)$ topological characteristic) nets, which are formed possibly by tetrahedral and octahedral building blocks [30,31]. So the topological type of unitary net is determined by the local geometry of node, which is related to the MBBs.

On the other hand, the phenomenon of interpenetration, once a rarity, is now becoming increasingly common aided by the rapid growth of network-based crystal engineering [32–34]. The origin of interpenetration can be ascribed to the presence of large free voids in a single network, though it has been demonstrated that interpenetration does not prevent the possibility of obtaining open porous materials [35–38]. In consequence of mother nature's *horror vacui*, such a crystal structure with extra-large pores is

* Corresponding authors.
E-mail addresses: zmsu@nenu.edu.cn (Z.-M. Su), lishunli@yahoo.cn (S.-L. Li).

0022-4596/$ - see front matter © 2009 Elsevier Inc. All rights reserved.
doi:10.1016/j.jssc.2009.08.018

unstable except by inclusion of suitable guests or by further interpenetration [39–40]. The degrees of interpenetration have consanguineous relation with the sizes of void, which is determined possibly by the length of ligand [41–42].

As shown above, in order to control the network formation we have to answer two questions prior to the preparation: (1) What kind of nets can be constructed from various molecular building blocks? (2) Do these nets interpenetrate, and what is the possible reason about the degrees of interpenetration? In this paper, we will consider above-mentioned questions and construct the 3D interpenetrating nets based on tetrahedral and octahedral building blocks. We will also investigate the relationship between topological types and molecular building blocks, and between the degrees of interpenetration and the ligands' length. To achieve this aim, we have designed and synthesized a series of flexible N-donor ligands (bpib and bib Chart 1) and multi-carboxylic bridging ligands (H_2L^1, H_2L^2 and H_2L^3). As an accurate prediction of the final structure is impossible, the exploration of the influencing factors for the ultimate structures is not trivial. In this paper, we have tried different synthetic conditions and performed many experiments. Fortunately, compounds $[Cd(bpib)_{0.5}(L^1)]$ (**1**), $[Cd(bpib)_{0.5}(L^2)]\cdot H_2O$ (**2**), $[Cd(bpib)_{0.5}(L^3)]$ (**3**) and $[Cd(bib)_{0.5}(L^1)]$ (**4**) have been successfully isolated by hydrothermal methods. In addition, the infrared spectra, thermogravimetric analyses and the luminescent properties of these compounds have been investigated in detail.

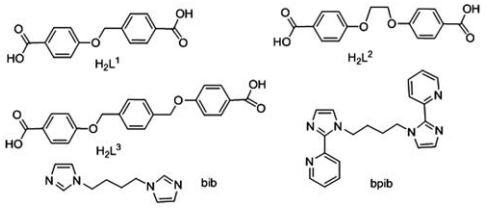

Chart 1. Four kinds of carboxylate ligands and two kinds of neutral ligands in **1**–**4**.

2. Experimental section

2.1. Materials and measurements

Chemicals were purchased from commercial sources and used without further purification, bpib, bib and H_2L^2 were prepared according to the literatures [43–46]. The C, H, and N elemental analysis was conducted on a Perkin–Elmer 240C elemental analyzer. The FT-IR spectra were recorded from KBr pellets in the range of 4000–400 cm^{-1} on a Mattson Alpha-Centauri spectrometer. TGA was performed on a Perkin–Elmer TG-7 analyzer heated from room temperature to 600 °C under nitrogen. The solid-state emission/excitation spectra were recorded on a Varian Cary Eclipse spectrometer at room temperature.

2.2. Synthesis of H_2L^1

A mixture of ethyl 4-hydroxybenzoate (8.30 g, 50 mmol) and NaOH (2.00 g, 50 mmol) in DMSO (20 mL) was stirred at 5 °C for 2 h, then 4-(chloromethyl)benzonitrile (7.55 g, 50 mmol) was added. The mixture was cooled to room temperature after stirring at 50 °C for 24 h, and then poured into 200 mL of water. A yellow solid of ethyl 4-(4-cyanobenzyloxy)benzoate formed immediately, which was isolated by filtration in 94% yield after drying in air.

A mixture of ethyl 4-(4-cyanobenzyloxy)benzoate (14.07 g, 50 mmol) and KOH (11.20 g, 200 mmol) in H_2O (200 mL) was stirred at 100 °C for 15 h, and was cooled to room temperature. Then the mixture was adjusted to pH ≈ 5 with HCl (1.0 mol L^{-1}), and a white solid of H_2L^1 formed immediately, which was isolated by filtration in 60% yield after drying in air. IR (cm^{-1}): 3743 (w), 3442 (w), 2985 (w), 2546 (w), 2362 (m), 1681 (s), 1606 (s), 1577 (m), 1514 (m), 1425 (s), 1385 (s), 1292 (s), 1252 (s), 1172 (s), 1047 (m), 949 (w), 854 (w), 765 (m).

2.3. Synthesis of H_2L^3

A mixture of ethyl 4-hydroxybenzoate (16.6 g, 100 mmol) and NaOH (4.00 g, 100 mmol) in DMSO (60 mL) was stirred at 5 °C for

Table 1
Crystal data and structure refinements for compounds **1**–**4**.

	1	2	3	4
Formula	$C_{25}H_{20}CdN_3O_5$	$C_{26}H_{24}CdN_3O_7$	$C_{32}H_{26}CdN_3O_6$	$C_{50}H_{48}Cd_2N_8O_{10}$
fw	554.84	602.88	660.96	1145.76
Crystal system	Monoclinic	Triclinic	Triclinic	Orthorhombic
Space group	$P2_1/n$	$P_{\bar{1}}$	$P_{\bar{1}}$	$P2_12_12$
a (Å)	9.0900(12)	9.0560(12)	9.1770(12)	14.3920(4)
b (Å)	23.9510(14)	11.191(11)	11.2110(15)	25.2960(9)
c (Å)	11.286(3)	15.264(2)	16.841(2)	6.9590(16)
α (deg)	90	102.263(2)	107.316(2)	90
β (deg)	108.500(2)	92.198(3)	91.370(2)	90
γ (deg)	90	108.628(2)	108.692(2)	90
V (Å^3)	2330.2(7)	1423.0(14)	1553.2(4)	2533.5(6)
Z	4	2	2	2
Mu (mm^{-1})	0.979	0.812	0.749	0.904
$D_{calcd.}$ ($g\,cm^{-3}$)	1.582	1.407	1.413	1.502
F (000)	1116	610	670	1160
Reflns collected/unique	1569/4157	8661/6356	9361/6860	15421/6097
R (int)	0.0594	0.0879	0.0256	0.0468
GOF on F^2	1.028	1.055	0.977	0.966
R_1[a] [$I>2\sigma(I)$]	0.0477	0.0879	0.0557	0.0577
wR_2[b][$I>2\sigma(I)$]	0.1110	0.2335	0.1257	0.1503
wR_2 for all data	0.1247	0.2462	0.1456	0.1652
Largest residuals [e Å^{-3}]	0.906/−0.547	1.940/−0.995	0.490/−0.654	1.444/−0.798

[a] $R_1=\Sigma||F_o|-|F_c||/\Sigma|F_o|$.
[b] $wR_2=|\Sigma w(|F_o|^2-|F_c|^2)|/\Sigma|w(F_o^2)^2|^{1/2}$.

2 h, then 1,4-bis(chloromethyl)benzene (8.75 g, 50 mmol) was added. The mixture was cooled to room temperature after stirring at 50 °C for 24 h, and then poured into 200 mL of water. A yellow solid of diethyl 4,4′-(1,4-phenylenebis(methylene))bis(oxy)dibenzoate formed immediately, which was isolated by filtration in 88% yield after drying in air.

A mixture of diethyl 4,4′-(1,4-phenylenebis(methylene))bis(oxy)dibenzoate (21.7 g, 50 mmol) and KOH (11.20 g, 200 mmol) in H_2O (300 mL) was stirred at 100 °C for 15 h, and was cooled to room temperature. Then the mixture was adjusted to pH ≈ 5 with HCl (1.0 mol L^{-1}), and a white solid of H_2L^3 formed immediately, which was isolated by filtration in 59% yield after drying in air. IR (cm^{-1}): 3551 (w), 3413 (w), 2980 (w),1701 (s), 1637 (m), 1604 (s), 1578 (m), 1508 (m), 1480 (m), 1423 (w), 1367(w), 1277 (s), 1254 (s), 1173 (s), 1114 (m), 1020 (m), 868 (w), 848 (m), 771 (w).

2.4. Synthesis of $[Cd(bpib)_{0.5}(L^1)]$ (1)

A mixture of bpib (0.34 g, 1.0 mmol), H_2L^1 (0.27 g, 1.0 mmol), $Cd(OAc)_2 \cdot 2H_2O$ (0.27 g, 1.0 mmol), NaOH (0.08 g, 2.0 mmol) and H_2O (10 mL) was stirred for 1 h and then sealed in a 25 mL Teflonlined stainless steel container. The container was heated to 150 °C and held at that temperature for 72 h, then cooled to 100 °C at a rate of 10 °C h^{-1}, and held for 8 h, followed by further cooling to 30 °C at a rate of 5 °C h^{-1}. Colorless crystals of **1** were collected in 71% yield based on $Cd(OAc)_2 \cdot 2H_2O$. Anal. Calcd. for $C_{25}H_{20}CdN_3O_5$ (554.84): C, 54.12; H, 3.63; N, 7.57. Found: C, 54.05; H, 3.55; N, 7.63%. IR (cm^{-1}): 3425 (s), 3121 (w), 2940 (w), 1595 (s), 1546 (m), 1468 (s), 1397 (s), 1249 (m), 1168 (w), 787 (m), 745 (m), 698 (m), 628 (w).

2.5. Synthesis of $[Cd(bpib)_{0.5}(L^2)] \cdot H_2O$ (2)

A mixture of bpib (0.34 g, 1.00 mmol), H_2L^2 (0.30 g, 1.0 mmol), $Cd(OAc)_2 \cdot 2H_2O$ (0.27 g, 1.0 mmol), NaOH (0.08 g, 2.0 mmol) and H_2O (10 mL) was stirred for 1 h and then sealed in a 25 mL Teflonlined stainless steel container. The container was heated to 150 °C and held at that temperature for 72 h, then cooled to 100 °C at a rate of 10 °C h^{-1}, and held for 8 h, followed by further cooling to 30 °C at a rate of 5 °C h^{-1}. Colorless crystals of **2** were collected in 66% yield based on $Cd(OAc)_2 \cdot 2H_2O$. Anal. Calcd. for $C_{26}H_{24}CdN_3O_7$ (602.88): C, 51.80; H, 4.01; N, 6.97. Found: C, 51.79; H, 3.98; N, 6.86%. IR (cm^{-1}): 3423 (s), 2935 (m), 1604 (s), 1511 (m), 1467 (m), 1396 (s), 1302 (m), 1248 (s), 1171 (m), 1109 (m), 1062 (w), 934 (w), 784 (m), 700 (w), 666 (w).

2.6. Synthesis of $[Cd(bpib)_{0.5}(L^3)]$ (3)

A mixture of bpib (0.34 g, 1.00 mmol), H_2L^4 (0.38 g, 1.00 mmol), $Cd(OAc)_2 \cdot 2H_2O$ (0.27 g, 1.0 mmol), NaOH (0.08 g, 2.00 mmol) and H_2O (10 mL) was stirred for 1 h and then sealed in a 25 mL teflonlined stainless steel container. The container was heated to 150 °C and held at that temperature for 72 h, then cooled to 100 °C at a rate of 10 °C h^{-1}, and held for 8 h, followed by further cooling to 30 °C at a rate of 5 °C h^{-1}. Colorless crystals of **3** were collected in 74% yield based on $Cd(OAc)_2 \cdot 2H_2O$. Anal. Calcd. for $C_{32}H_{26}CdN_3O_6$ (660.96): C, 58.15; H, 3.96; N, 6.35. Found: C, 58.03; H, 4.01; N, 6.39%. IR (cm^{-1}): 3421 (m), 3105 (m), 2932 (m), 1598 (s), 1546 (s), 1469 (m), 1385 (s), 1300 (w), 1243 (s), 1167 (m), 1102 (w), 853 (w), 699 (w), 643 (w).

2.7. Synthesis of $[Cd(bib)_{0.5}(L^1)]$ (4)

A mixture of bib (0.19 g, 1.00 mmol), H_2L^2 (0.27 g, 1.0 mmol), $Cd(OAc)_2 \cdot 2H_2O$ (0.27 g, 1.0 mmol), NaOH (0.08 g, 2.00 mmol) and H_2O (10 mL) was stirred for 1 h and then sealed in a 25 mL teflonlined stainless steel container. The container was heated to 150 °C and held at that temperature for 72 h, then cooled to 100 °C at a rate of 10 °C h^{-1}, and held for 8 h, followed by further cooling to 30 °C at a rate of 5 °C h^{-1}. Colorless crystals of **4** were collected in 78% yield based on $Cd(OAc)_2 \cdot 2H_2O$. Anal. Calcd. for $C_{50}H_{48}Cd_2N_8O_{10}$ (1145.76): C, 52.41; H, 4.22; N, 9.78. Found: C, 52.39; H, 4.19; N, 9.74%. IR (cm^{-1}): 3424 (m), 3122 (m), 2936 (w), 1595 (w), 1511 (s), 1466 (m), 1396 (m), 1271 (w), 1228 (s), 1108 (s), 1080 (s), 834 (m), 737 (s), 657 (m).

2.8. X-ray crystallography

Single-crystal X-ray diffraction data for compounds **1**–**4** were recorded on a Bruker Apex CCD diffractometer with graphite-monochromated MoK_α radiation (λ=0.71073 Å) at 293 K. Absorption corrections were applied using multi-scan technique. All the structures were solved by Direct Method of SHELXS-97 [47] and refined by full-matrix least-squares techniques using the SHELXL-97 program [48] within WINGX [49]. Non-hydrogen atoms were refined with anisotropic temperature parameters. The hydrogen atoms of the organic ligands were refined as ideal positions. H atoms of water molecules were located from different Fourier maps. The detailed crystallographic data and structure refinement parameters for **1**–**4** are summarized in Table 1. CCDC-718526 (for 1), -718527 (for 2), -718528 (for 3), -718529 (for 4) contain the supplementary crystallographic data for this paper. These data can

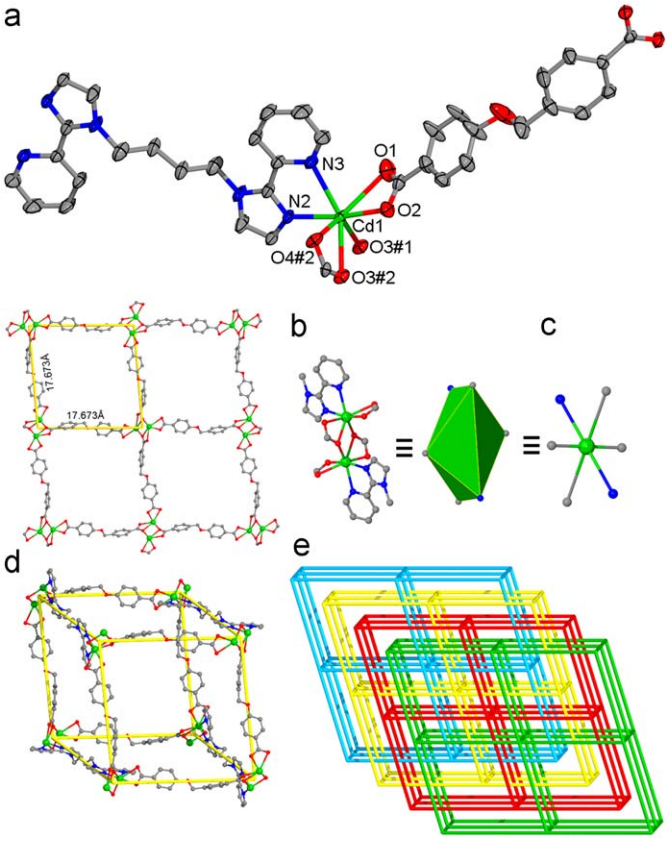

Fig. 1. (a) Coordination environment of Cd^{II} atom in **1** with the ellipsoids drawn at the 30% probability level, hydrogen atoms were omitted for clarity. (b) Ball-and-stick representation of the sheet-like structure of compound **1**. (c) Schematic representation of the six-connected unit with octahedral building block. (d) Ball-and-stick representation of the dimensional sizes of the α-Po framework in **1**. (e) Schematic description of the interpenetrating nets of **1**.

be obtained free of charge from The Cambridge Crystallographic Data Centre via www.ccdc.cam.ac.uk/data_request/cif.

3. Results and discussion

3.1. Description of the crystal structures

3.1.1. Structure description of 1

The asymmetric unit of **1** is shown in Fig. 1a, which consists of one kind of unique Cd^{II} ion, one kind of bpib ligand and one kind of $(L^1)^{2-}$ anion, respectively. Each Cd1 center is in a distorted pentagonal bipyramidal coordination geometry, and is coordinated by five carboxylate oxygen atoms from three $(L^1)^{2-}$ anions and two nitrogen atoms from one bpib ligand. The Cd–O and Cd–N bond lengths are all within the normal ranges [50,51]. Each $(L^1)^{2-}$ anion with the (k^2)-$(k^2$-$\mu_2)$-μ_3 coordination mode (Chart S1a) connects the Cd^{II} ions in two directions to make up a 2D layer structure (Fig. 1b) with the grid showing the dimensional sizes of 17.673 Å × 17.673 Å, in which there is a $[Cd_2(-COO)_4]$ unit formed by four carboxylate groups and two Cd^{II} ions. The $[Cd_2(-COO)_4]$ unit can be regarded as an octahedral MBBs. The 2D layers are pillared by bpib ligands with the TTT (T=*trans*) conformation to form a 3D framework. If each $[Cd_2(-COO)_4]$ unit is considered as a six-connected node (Fig. 1c), the structure of **1** exhibits a α-Po topology (Fig. 1d).

Because of the spacious nature of the single network, the potential voids are filled via mutual interpenetration of identical 3D frameworks, generating a four-fold interpenetrating architecture (Fig. 1e).

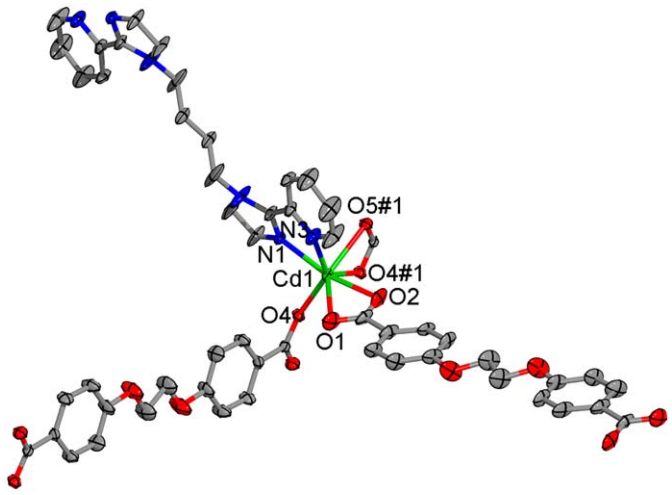

Fig. 2. Coordination environment of Cd^{II} atom in **2** with the ellipsoids drawn at the 30% probability level, hydrogen atoms and water molecule were omitted for clarity.

3.1.2. Structure description of 2

To evaluate the effects of different length of carboxylate anions on the various topologies, other two structurally related ligands H_2L^2 and H_2L^3 have been utilized, and two different frameworks have been isolated. When the more longer H_2L^2 ligand has been reacted with Cd^{II} and bpib, using a preparation procedure similar to that of **1** and resulting in a 3D four-fold interpenetrating network of **2**. As shown in Fig. 2, the structure of **2** contains one kind of unique Cd^{II} ion, one kind of bpib ligand and two kinds of $(L^2)^{2-}$ anions, respectively. Cd1 ion shows seven-coordinated pentagonal bipyramidal geometry which is surrounded by five carboxylate oxygen atoms from three $(L^2)^{2-}$ anions and two nitrogen atoms from one bpib ligand. Two kinds of $(L^2)^{2-}$ anions with two types of coordination modes; namely, $(k^2$-$\mu_2)$-$(k^2$-$\mu_2)$-μ_4 and (k^2)-(k^2)-μ_2 (Chart S1c and d), link all Cd^{II} ions to generate a 2D sheet with the grid showing the dimensional sizes of 18.044 Å × 21.518 Å (Fig. S1a). And there exists a $[Cd_2(-COO)_4]$ unit formed by four carboxylate groups and two Cd^{II} ions in the sheet. The 2D layers are pillared by bpib ligands with the TTT conformation to form a 3D framework. If each $[Cd_2(-COO)_4]$ unit is considered as a six-connected node, the structure of **2** exhibits a α-Po topology (Figs. S1b and c).

In addition, other three identical 3D frameworks interpenetrate one 3D framework to generate a four-fold interpenetrating architecture. Compounds **1** and **2** are both four-fold interpenetrating frameworks which are similar to the reported compounds $[Zn_4(\mu_4\text{-}O)(L_1)_6(DMF)_2]\cdot 4DMF\cdot 3CH_3OH\cdot 2H_2O$ [52,53] and $[Zn_4(\mu_4\text{-}O)(L_2)_3]\cdot 5DMF\cdot 5C_2H_5OH\cdot H_2O$ [18a] (H_2L_1=6,6′-dichloro-2,2′-diethoxy-1,1′-binaphthyl-4,4′-dibenzoic acid and H_2L_2=6,6′-dichloro-2,2′-dibenzyloxy-1,1′-binaphthyl-4,4′-dibenzoic acid), and 2,2′,6,6′-tetramethyl-4,4′-terphenyldiol [53].

3.1.3. Structure description of 3

When using longer H_2L^3 ligand instead of H_2L^2 ligand, compound **3** with different structural type from others has been obtained. Single crystal X-ray analysis reveals that compound **3** is constructed by one kind of Cd^{II} ion, two kinds of $(L^3)^{2-}$ anions and one bpib ligand (Fig. 3a). Four carboxylate groups from different $(L^3)^{2-}$ anions coordinate to two Cd^{II} ions to form a $[Cd_2(-COO)_4]$ unit which is linked by two kinds of $(L^3)^{2-}$ anions with $(k^2$-$\mu_2)$-

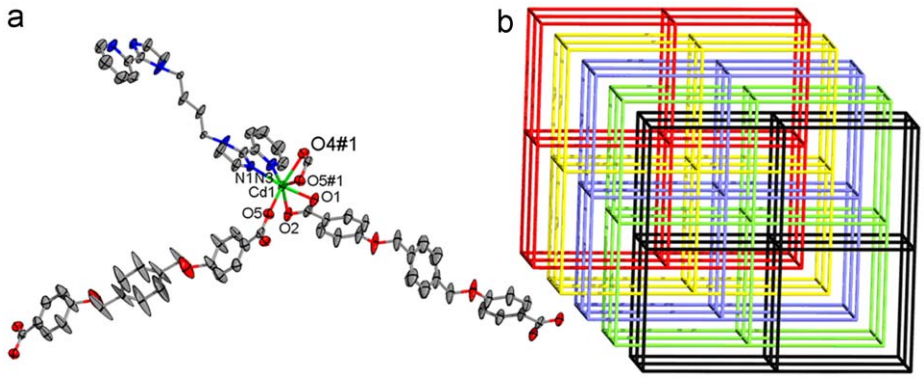

Fig. 3. (a) Coordination environment of Cd^{II} atom in **3** with the ellipsoids drawn at the 30% probability level, hydrogen atoms were omitted for clarity. (b) Schematic description of the interpenetrating α-Po nets of **3**.

(k^2-μ_2)-μ_4 and (k^2)-(k^2)-μ_2 (Chart S1e and f) coordination modes to generate a 2D sheet, showing a large window with the dimensional sizes of 22.071 Å × 25.205 Å (Fig. S2a), which is larger than those in compounds **1** and **2**. The 2D layers are pillared by bpib ligands with the TTT conformation to form a 3D framework. If each [Cd_2(–COO)$_4$] unit is considered as a six-connected node, the structure of **3** exhibits a α-Po topology (Figs. 3b and S2b).

Because of the larger sizes of the single network than those in compounds **1** and **2**, there are other four identical 3D frameworks interpenetrate one 3D framework to generate a five-fold interpenetrating architecture. To our best knowledge, compound **3** is the first example of the five-fold interpenetrating α-Po architecture.

Comparing the structures of **1**, **2** and **3**, there are the similar MBBs of [Cd_2(–COO)$_4$] formed by two Cd^{II} ions and four carboxylate anions, which may be caused by the similar coordination modes (k^2-μ_2) of carboxylate groups. Then [Cd_2(–COO)$_4$] MBBs are connected by various carboxylate anions to generate grids with different sizes based on the distinct multi-carboxylate lengths. In **1**, the dimensional sizes (*a* and *b*) of the grids are 17.673 Å × 17.673 Å, and those in compounds **2** and **3** are 18.044 Å × 21.518 Å and 22.071 Å × 25.205 Å, respectively. Being connected by four –(CH_2)– groups, the flexible neutral bpib ligand is selected to construct compounds **1**–**3** with different torsion angles and alterable distances (*c*) between two metal centers coordinated by one bpib ligand, which can benefit above mentioned requirement. The sheets are pillared by bpib ligands with the distances between two metal centers of 14.624, 14.627 and 14.668 Å in **1**–**3**, respectively. From the theoretic view, the longer the distances of *a*, *b* and *c* are, the higher the degrees of interpenetration for α-Po topology exhibit. Based on the above discussion, the values of *a*, *b* and *c* in compound **3** is higher than those in compounds **1** and **2**, so compounds **1** and **2** show the four-fold interpenetrating α-Po topologies and compound **3** exhibits a five-fold interpenetrating α-Po net. So we have achieved the transformation about the degrees of interpenetration via changing the length of carboxylate ligands in α-Po topological nets when using similar MBBs. These results indicate the structures with different degrees of interpenetration can be designed and synthesized in the crystal engineering.

3.1.4. Structure description of 4

The above mentioned results encouraged us to expand our studies to the other topological structural types. In order to obtain the four-connected net, we select the bib instead of bpib ligand. Compared with 2-(2-pyridyl)imidazole group of bpib, the imidazole group of bib has smaller steric hindrance when coordinates to the same metal center.

It is interesting that bib is selected to react with Cd^{II} ion and H_2L^1, different topological structure of **4** has been obtained. Single crystal X-ray analysis reveals that compound **4** contains one kind of Cd^{II} ion, one kind of $(L^1)^{2-}$ anion and one bib ligand (Fig. 4a). Cd^{II} ion is surrounded by four carboxylate oxygen atoms from two $(L^1)^{2-}$ anions and two nitrogen atoms from different bib ligands, which can be regarded as a tetrahedral MBBs. Each $(L^1)^{2-}$ anion shows a (k^2)-(k^2)-μ_2 coordination mode (Chart S1b) and connects Cd^{II} ions to generate a wavelike chain (Fig. 4b), which is linked by bib ligand with the TTT coordination conformation to form a 3D framework (Fig. 4c and d). From the topological view, if each tetrahedral MBB is considered as a four-connected node, and $(L^1)^{2-}$ and bib ligands are considered as linkages, the structure of **4** is a diamond topology (Scheme 1).

In consequence of mother nature's *horror vacui*, other five identical frameworks interpenetrate one net to generate an interesting six-fold interpenetrating net (Fig. 4e and f).

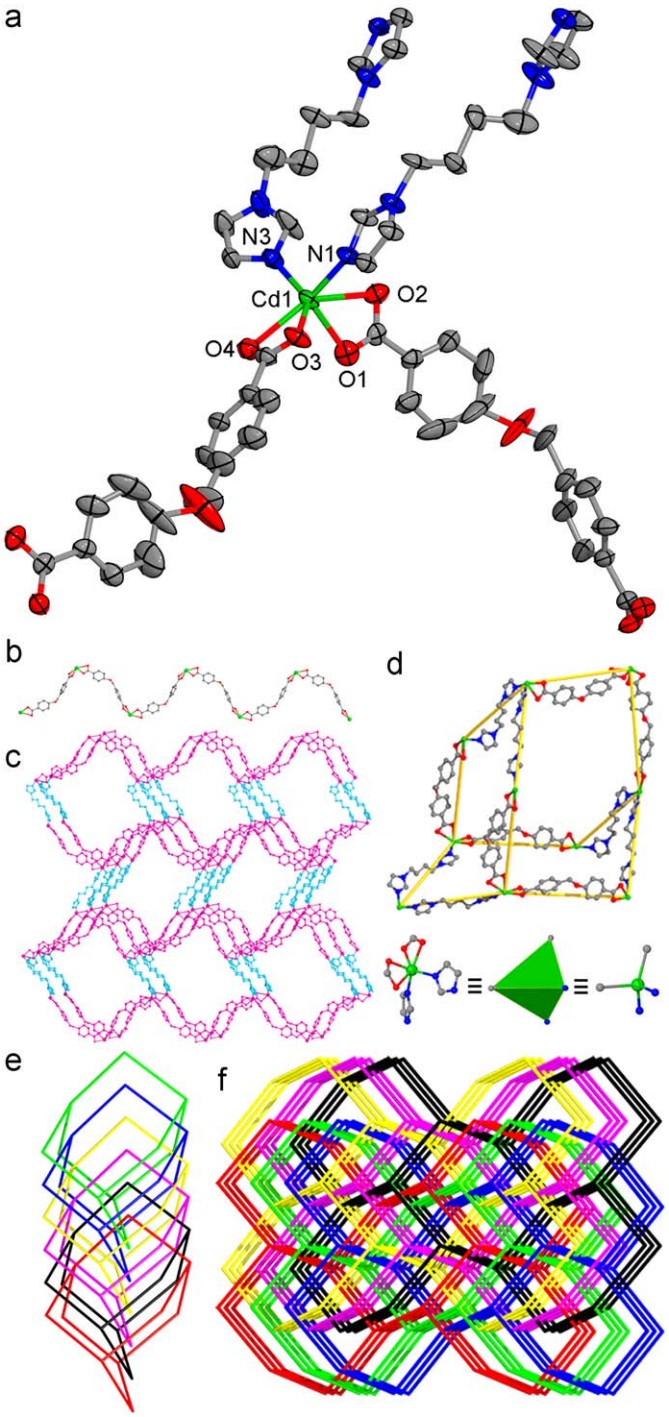

Fig. 4. (a) Coordination environment of Cd^{II} atom in **4** with the ellipsoids drawn at the 30% probability level, hydrogen atoms were omitted for clarity. (b) Ball-and-stick representation of the chain-like structure of compound **4**. (c) Ball-and-stick representation of the 3D framework of compound **4**. (d) Ball-and-stick representation of the dimensional sizes of the diamondoid framework of **4**. (e) and (f) Schematic description of the interpenetrating nets of **4**.

By careful inspection of compounds **1**–**4**, **1**–**3** are six-connected α-Po nets constructed by octahedral [Cd_2(–COO)$_4$] MBBs. When selecting smaller steric hindrance bib ligand, the four-connected diamondoid net is formed by tetrahedral MBBs in **4**. These results indicate that various MBBs can be constructed by changing different ligands and metal centers. The topological types of unitary nets are determined by these MBBs with various polygons or polyhedra. Such as four- and six-connected topologies are

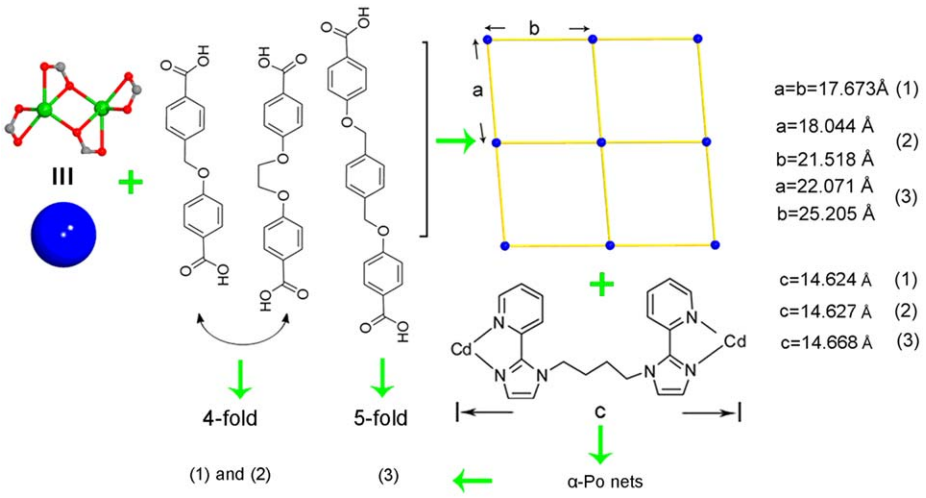

Scheme 1. The relationship between the degrees of interpenetration and the ligands' length about **1**–**3**.

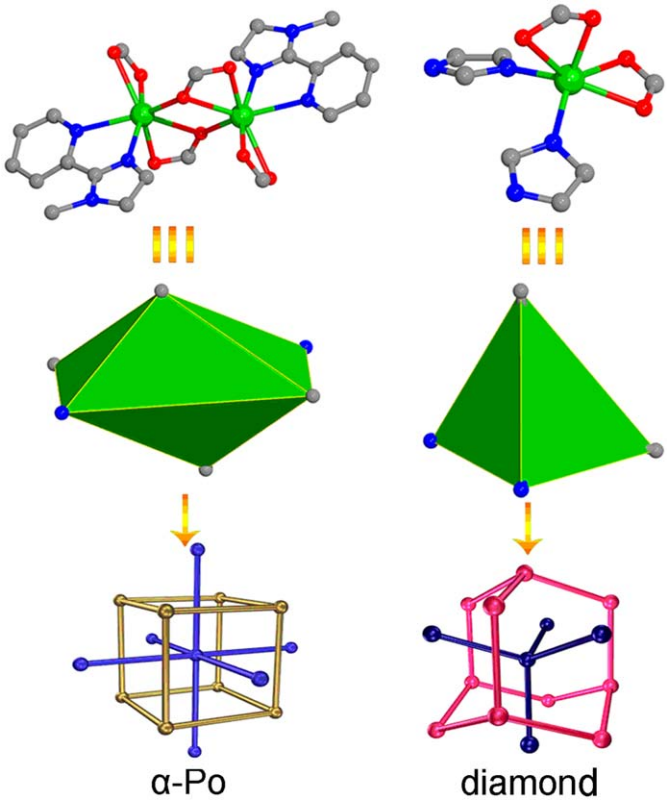

Scheme 2. Schematic representation of MBBs and six- and four-topological nets.

formed by tetrahedral and octahedral building blocks in above-mentioned compounds. The structures of compounds **1** and **4** show various topological types with different degrees of interpenetration by using different carboxylate acids and neutral ligands with similar length. The different degrees of interpenetration maybe caused by different sizes of free voids in a single network, which is determined possibly by the shortest cycle in different topological types. Compounds **1** and **4** exhibit four-fold α-Po net and six-fold diamondoid net, respectively, the increase about the degrees of interpenetration can be ascribed to above-mentioned viewpoints (Scheme 2).

3.2. FT-IR spectra

In the IR spectra of complexes **1–4**, the characteristic bands of the carboxylate groups appeared in the usual region at 1595 cm^{-1} (**1**), 1604 cm^{-1} (**2**), 1598 cm^{-1} (**3**) and 1595 cm^{-1} (**4**) for the antisymmetric stretching vibrations and at 1397 cm^{-1} (**1**), 1396 cm^{-1} (**2**), 1385 cm^{-1} (**3**) and 1396 cm^{-1} (**4**) for the symmetric stretching vibrations, respectively. The separation (Δv) between v_{asym} (COO^-) and v_{sym} (COO^-) is 198, 208, 213 and 199 cm^{-1} for **1**, **2**, **3**, **4**, respectively, indicating bidentate coordination of the carboxylate groups in such complexes. The absence of the strong carboxyl absorption band around 1730 cm^{-1} of multicarboxylate acid indicates the complete deprotonation. Weak absorptions observed over the range 2900–2950 cm^{-1} can be attributed to the v_{CH_2} of the $(L^1)^{2-}$, $(L^2)^{2-}$ and $(L^3)^{2-}$ ligands. The bands at 1468 cm^{-1} for **1**, 1467 cm^{-1} for **2**, 1469 cm^{-1} for **3** and 1466 cm^{-1} for **4** are typical for v (C═N) of the imidazole ring [54]. These spectral characteristics are consistent with the following X-ray structure analyses.

3.3. Thermal analysis

In order to characterize the compounds more fully in terms of thermal stability, their thermal behaviors were studied by TGA. The experiments were performed on samples consisting of numerous single crystals of **1–4** under N_2 atmosphere with a heating rate of 10 °C/min. As shown in Figs. S3 in the supporting information (Table 2).

For **1**, the weight loss begins to decompose at 197 °C and ends above 548 °C. The remaining weight of 23.4% corresponds to the percentage (23.1%) of CdO. The TGA curve of **2** shows that it loses the water molecules from room temperature to 109 °C (obsd. 2.7%, calcd. 3.0%), and then the anhydrous compound begins to decompose, leading to the formation of CdO as the residue (obsd. 21.5%, calcd. 21.4%). For compounds **3** and **4**, the weight losses in the range of 211–541 °C for **3** and 233–526 °C for **4** correspond to the removal of the corresponding organic components, and the remaining weight corresponds to the formation of CdO in **3** (obsd. 19.5%, calcd. 19.4%) and CdO in **4** (obsd. 22.7%, calcd. 22.4%).

3.4. Luminescent properties

Luminescent compounds are of great current interest because of their various applications in chemical sensors, photochemistry

Table 2
The TG of compounds **1**–**4**.

	1 Step	2 Step	Remaining component
1	197–548 °C obsd. 76.6%, calcd. 76.9%		CdO obsd. 23.4%, calcd. 23.1%
2	rt-109 °C obsd. 2.7%, calcd. 3.0%	205–518 °C obsd. 75.8%, calcd. 75.6%	CdO obsd. 21.5%, calcd. 21.4%
3	211–541 °C obsd. 80.5%, calcd. 80.6%		CdO obsd. 19.5%, calcd. 19.4%
4	233–526 °C obsd. 78.3%, calcd. 78.6%		CdO obsd. 22.7%, calcd. 22.4%

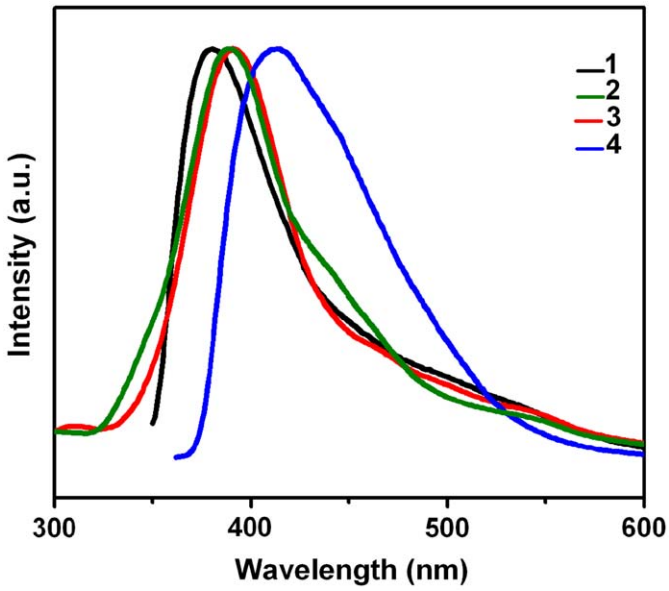

Fig. 5. Solid-state photoluminescent spectra of **1**–**4** at room temperature.

and electroluminescent display [55–57]. The main emission peaks of bpib and bib are at 532 and 436 nm (λex=370 and 380 nm), respectively, which may be attributed to the $\pi^* \rightarrow \pi$ transition [53]. And solid H_2L^1–H_2L^3 ligands are nearly nonfluorescent in the range 300–700 nm at ambient temperature. The excitation leads to intense emission bands at 379 nm for **1** (λex=370 nm), 389 nm for **2** (λex=285 nm), 391 nm for **3** (λex=280 nm) and 413 nm for **4** (λex=290 nm), respectively (Fig. 5 and Table 3). In comparison with the free ligands, the emission maxima of compounds **1**–**4** have changed, which may be attributed to a joint contribution of the intraligand transitions and/or charge transfer transitions between the coordinated ligands and the metal center [44,50,58–61].

4. Conclusion

In summary, we have synthesized four mixed-ligand coordination complexes under hydrothermal conditions. By careful inspection of these structures, we find that various carboxylic ligands and N-donor ligands with different coordination modes and conformations, and metal centers with different coordination geometries are important for the formation of the different MBBs. It is believed that the different topological types lie on different MBBs with various polygons or polyhedra. Such as four- and six-connected topologies are formed by tetrahedral and octahedral building blocks. In addition, with the increase of carboxylic ligands' length, the degrees of interpenetration have been changed in the α-Po topological nets. The successful isolation of these compounds not only provides intriguing examples of interpenetrating topology but also confirms that the simple unitary net can be designed and synthesized from specific MBBs with homologous polygons or polyhedra. Appropriate choices of carboxylic ligands and N-donor ligands as well as spatial linkers and metal centers with different coordination geometries will lead to the rational design and assembly of MOFs with well-regulated network structures.

Table 3
The wavelengths of the emission maximums and excitation (nm).

	bpib	bib	**1**	**2**	**3**	**4**
λem	532	36	379	389	391	413
λex	370	380	290	285	280	290

Acknowledgments

The authors gratefully acknowledge the financial support from the National Natural Science Foundation of China (Project nos. 20573016, 20901014 and 20703008), ChangJiang Scholars Program (2006), Program for Changjiang Scholars and Innovative Research Team in University (IRT0714), the National High-tech Research and Development Program (863 Program 2007AA03Z354), Department of Science and Technology of Jilin Province (20082103), the Science Foundation for Young Teachers of NENU (No. 20090407), the Science Foundation for Young of Jilin Scientific Development Project (nos. 20090125 and 20090129), and the Training Fund of NENU's Scientific Innovation Project (NENU-STC08019).

Appendix A. Supplementary material

Supplementary data associated with this article can be found in the online version at doi:10.1016/j.jssc.2009.08.018.

References

[1] O.M. Yaghi, M. O'Keeffe, N.W. Ockwig, H.K. Chae, M. Eddaoud, J. Kim, Nature 423 (2003) 705–714.
[2] A.J. Blake, N.R. Champness, P. Hubberstey, W.S. Li, M.A. Withersby, M. Schröder, Coord. Chem. Rev. 183 (1999) 117–138.
[3] P.J. Hagrman, D. Hagrman, J. Zubieta, Angew. Chem. Int. Ed. 38 (1999) 2638–2684.
[4] Y.Q. Lan, S.L. Li, X.L. Wang, Z.M. Su, K.Z. Shao, E.B. Wang, Chem. Commun. (2007) 486–487.
[5] O.R. Evans, W. Lin, Acc. Chem. Res. 35 (2002) 511–522;
S.L. James, Chem. Soc. Rev. 32 (2003) 276–288.

[6] O. Delgado-Friedrichs, M.D. Foster, M. O'Keeffe, D.M. Prosperio, M. Treacy, O.M. Yaghi, J. Solid State Chem. 178 (2005) 2533–2554.
[7] R. Natarajan, G. Savitha, P. Dominiak, K. Wozniak, J.N. Moorthy, Angew. Chem. Int. Ed. 44 (2005) 2115–2119.
[8] R. Robson, J. Chem. Soc. Dalton Trans. (2000) 3735–3744.
[9] S. Han, J.V. Smith, Acta Crystallogr. Sect. A 55 (1999) 332–341.
[10] M. O'Keeffe, M. Eddaoudi, H. Li, T. Reineke, O.M. Yaghi, J. Solid State Chem. 152 (2000) 3–20.
[11] K. Biradha, CrystEngComm 5 (2003) 374–384.
[12] R.J. Hill, D.L. Long, N.R. Champness, P. Hubberstey, M. Schröder, Acc. Chem. Res. 38 (2005) 335–348.
[13] A.F. Wells, Three-dimensional Nets and Polyhedra, Wiley, New York, 1977.
[14] A.F. Wells, Further Studies of Three-dimensional Nets, ACA Monograph 8, American Crystallographic Association, 1979.
[15] B. Moulton, M.J. Zaworotko, Chem. Rev. 101 (2001) 1629–1658.
[16] M. Eddaoudi, D.B. Moler, H. Li, B. Chen, T.M. Reineke, M. O'Keeffe, O.M. Yaghi, Acc. Chem. Res. 34 (2001) 319–330.
[17] A. Erxleben, Coord. Chem. Rev. 246 (2003) 203–228.
[18] S. Kitagawa, R. Kitaura, S. Noro, Angew. Chem. Int. Ed. 43 (2004) 2334–2375.
[19] C. Janiak, Dalton Trans. (2003) 2781–2804.
[20] D.J. Tranchemontagne, Z. Ni, M. O'Keeffe, O.M. Yaghi, Angew. Chem. Int. Ed. 47 (2008) 5136–5147.
[21] H. Furukawa, J. Kim, N.W. Ockwig, M. O'Keeffe, O.M. Yaghi, J. Am. Chem. Soc. 130 (2008) 11650–11661.
[22] Z. Wang, V.Ch. Kravtsov, M.J. Zaworotko, Angew. Chem. Int. Ed. 44 (2005) 2877–2880.
[23] B. Moulton, J. Lu, R. Hajndl, S. Hariharan, M.J. Zaworotko, Angew. Chem. Int. Ed. 41 (2002) 2821–2824.
[24] J.A. Real, E. Andres, M.C. Munoz, M. Julve, T. Granier, A. Bousseksou, F. Varret, Science 268 (1995) 265–267.
[25] S.R. Batten, B.F. Hoskins, R. Robson, Chem. Eur. J. 6 (2000) 156–161.
[26] L. Carlucci, N. Cozzi, G. Ciani, M. Moret, D.M. Proserpio, S. Rizzato, Chem. Commun. (2002) 1354–1355.
[27] S.W. Keller, S. Lopez, J. Am. Chem. Soc. 121 (1999) 6306–6307.
[28] S. Noro, S. Kitagawa, M. Kondo, K. Seki, Angew. Chem. Int. Ed. 39 (2000) 2082–2084.
[29] B. Moulton, J.J. Lu, M.J. Zaworotko, J. Am. Chem. Soc. 123 (2001) 9224–9225.
[30] O. Delgado-Friedrichs, M. O'Keeffe, O.M. Yaghi, Acta Crystallogr. A 62 (2006) 350–355.
[31] O. Delgado-Friedrichs, M. O'Keeffe, O.M. Yaghi, Acta Crystallogr. A 59 (2003) 22–27.
[32] S.R. Batten, R. Robson, Angew. Chem. Int. Ed. 37 (1998) 1460–1494.
[33] S.R. Batten, CrystEngComm 3 (2001) 67–73.
[34] V.A. Blatov, L. Carlucci, G. Ciani, D.M. Proserpio, CrystEngComm 6 (2004) 377–395.
[35] L. Carlucci, G. Ciani, D.M. Proserpio, Coord. Chem. Rev. 246 (2003) 247–289.
[36] T.M. Reineke, M. Eddaoudi, D.M. Moler, M. O'Keeffe, O.M. Yaghi, J. Am. Chem. Soc. 122 (2000) 4843–4844.
[37] M. Kondo, M. Shimamura, S.-I. Noro, S. Minakoshi, A. Asami, K. Seki, S. Kitagawa, Chem. Mater. 12 (2000) 1288–1299.
[38] L. Carlucci, G. Ciani, D.M. Proserpio, CrystEngComm 5 (2003) 269–279.
[39] X.L. Wang, C. Qin, E.B. Wang, Z.M. Su, Chem.-Eur. J. 12 (2006) 2680–2691.
[40] X.L. Wang, C. Qin, E.B. Wang, Z.M. Su, Chem. Commun. (2007) 4245–4247.
[41] L. Carlucci, G. Ciani, D.M. Proserpio, S. Rizzato, CrystEngComm (2002) 413–425.
[42] L. Carlucci, G. Ciani, D.M. Proserpio, S. Rizzato, Chem. Eur. J. 8 (2002) 1519–1523.
[43] S.L. Li, Y.Q. Lan, J.F. Ma, J. Yang, G.H. Wei, L.P. Zhang, Z.M. Su, Cryst. Growth Des. 8 (2008) 675–684.
[44] Y.Q. Lan, S.L. Li, K.Z. Shao, X.L. Wang, D.Y. Du, Z.M. Su, D.J. Wang, Cryst. Growth Des. 8 (2008) 3490–3492.
[45] Y.Q. Lan, Y.M. Fu, K.Z. Shao, Z.M. Su, Acta Crystallogr. E 62 (2006) 2586–2587.
[46] Z.Q. Xu, J.D. Xu, S.S. Ni, J. Anhui Univ. (1991) 79–86.
[47] G.M. Sheldrick, SHELXS-97 Programs for X-ray Crystal Structure Solution, University of Göttingen, Göttingen, Germany, 1997.
[48] G.M. Sheldrick, SHELXS-97 Programs for X-ray Crystal Structure Refinement, University of Göttingen, Göttingen, Germany, 1997.
[49] L.J. Farrugia, WINGX A Windows Program for Crystal Structure Analysis, University of Glasgow, Glasgow UK, 1988.
[50] S.L. Li, Y.Q. Lan, J.F. Ma, Y.M. Fu, J. Yang, G.J. Ping, J. Liu, Z.M. Su, Cryst. Growth Des. 8 (2008) 1610–1616.
[51] S.L. Li, Y.Q. Lan, J.S. Qin, J.F. Ma, Z.M. Su, Cryst. Growth Des. 8 (2008) 2055–2057.
[52] B. Kesanli, Y. Cui, M.R. Smith, E.W. Bittner, B.C. Bockrath, W. Lin, Angew. Chem. Int. Ed. 44 (2005) 72–75.
[53] S. Aitipamula, A. Nangia, Chem. Commun (2005) 3159–3161.
[54] X.-L. Liu, R. Zhao, X.-H. Liu, J.-J. Yue, Y.-X. Yin, Y. Sun, X. Zhang, Chinese J. Chem. 21 (2003) 1047–1053.
[55] J.E. McGarrah, Y.-J. Kim, M. Hissler, R. Eisenberg, Inorg. Chem. 40 (2001) 4510–4511.
[56] Q. Wu, M. Esteghamatian, N.X. Hu, Z. Popovic, G. Enright, Y. Tao, M. D'Iorio, S. Wang, Chem. Mater. 12 (2000) 79–83.
[57] G.D. Santis, L. Fabbrizzi, M. Licchelli, A. Poggi, A. Taglietti, Angew Chem. Int. Ed. Engl. 35 (1996) 202–204.
[58] S.L. Zheng, J.H. Yang, X.L. Yu, X.M. Chen, W.T. Wong, Inorg. Chem. 43 (2004) 830–838.
[59] B. Valeur, Molecular Fluorescence: Principles and Applications, Wiley-VCH, Weinheim, 2002.
[60] A.W. Adamson, P.D. Fleischauer, Concepts of Inorganic Photochemistry, Wiley, New York, 1975.
[61] H. Yersin, A. Vogler, Photochemistry and Photophysics of Coordination Compounds, Springer, Berlin, 1987.